

Supplemental Appendix for “Severe Weather and the Macroeconomy”

Hee Soo Kim, Christian Matthes, Toan Phan

January 30, 2025

A.3 Omitted Robustness Check Figures

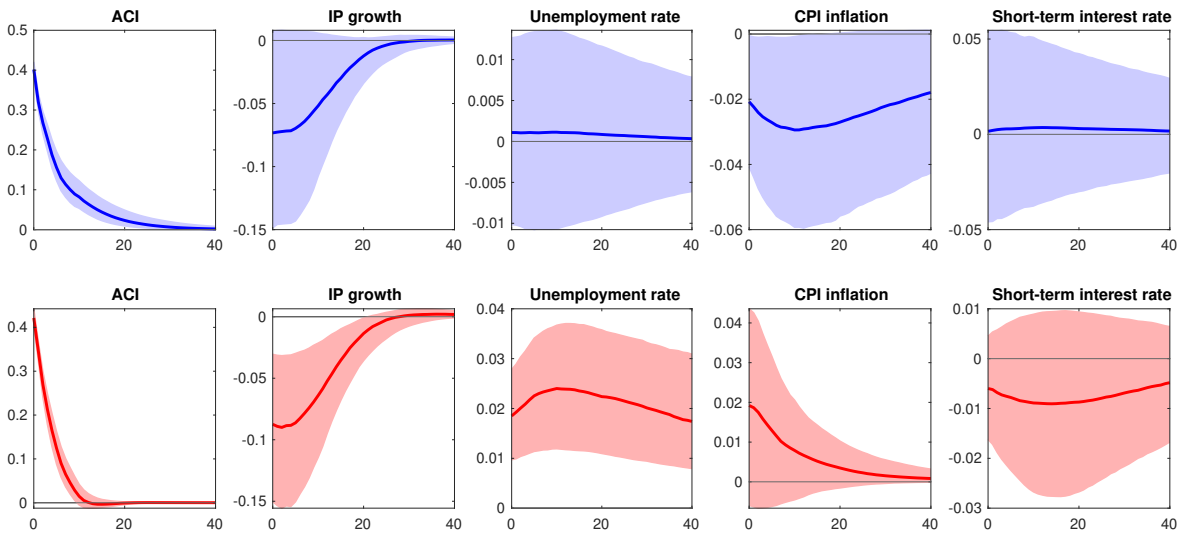


Figure A.1: Sample splitting: Impulse responses to a one-standard-deviation shock to the ACI. Top panels: $\tilde{z}_t = 0$ in 1963m4-1990m12; bottom panels: $\tilde{z}_t = 1$ in 1991m1-2019m5. Shaded areas represent 68% posterior bands. Horizontal axis: months after the ACI shock.

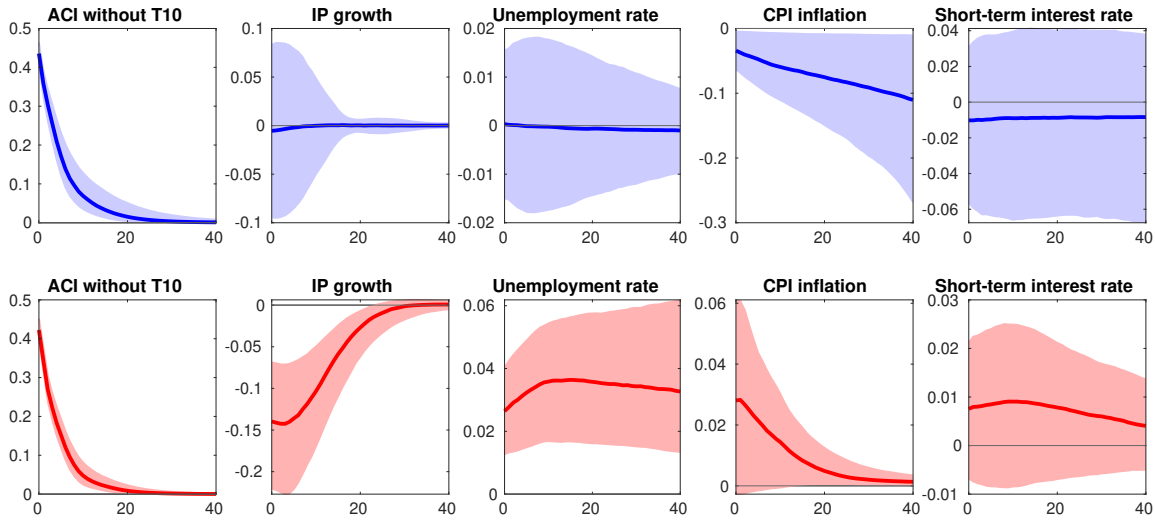


Figure A.2: Impulse responses to a one-standard-deviation shock to the ACI without $T10$. Top panels: beginning of sample ($\tilde{z}_t = 0$); bottom panels: end of sample ($\tilde{z}_t = 1$). Shaded areas represent 68% posterior bands. Horizontal axis: months after the ACI shock.

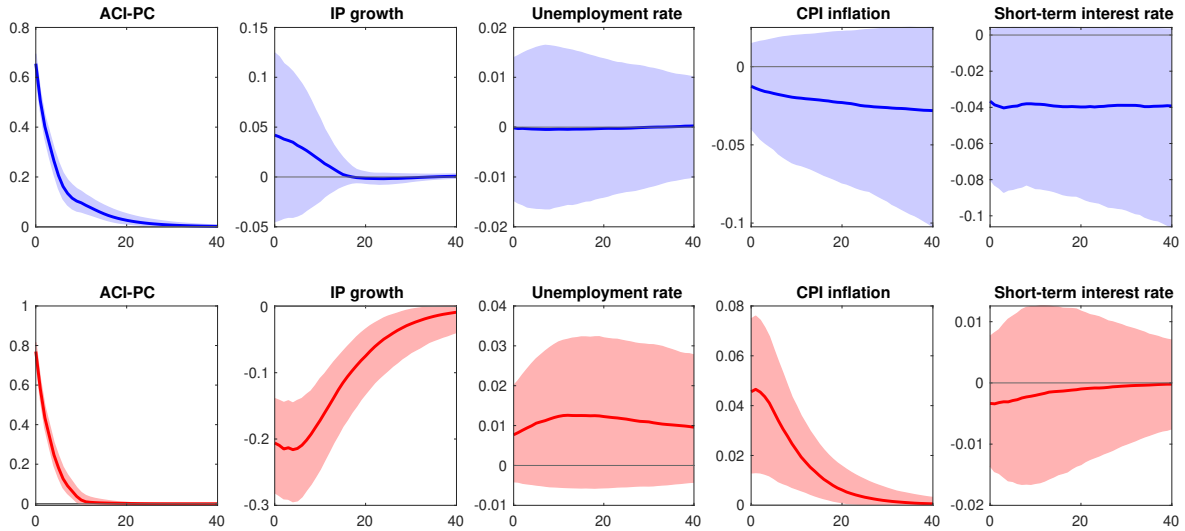


Figure A.3: Impulse responses to a one-standard-deviation shock to ACI-PC, which is the first principal component of disaggregated ACI component data. Top panels: beginning of sample ($\tilde{z}_t = 0$); bottom panels: end of sample ($\tilde{z}_t = 1$). Shaded areas represent 68% posterior bands. Horizontal axis: months after the ACI shock.

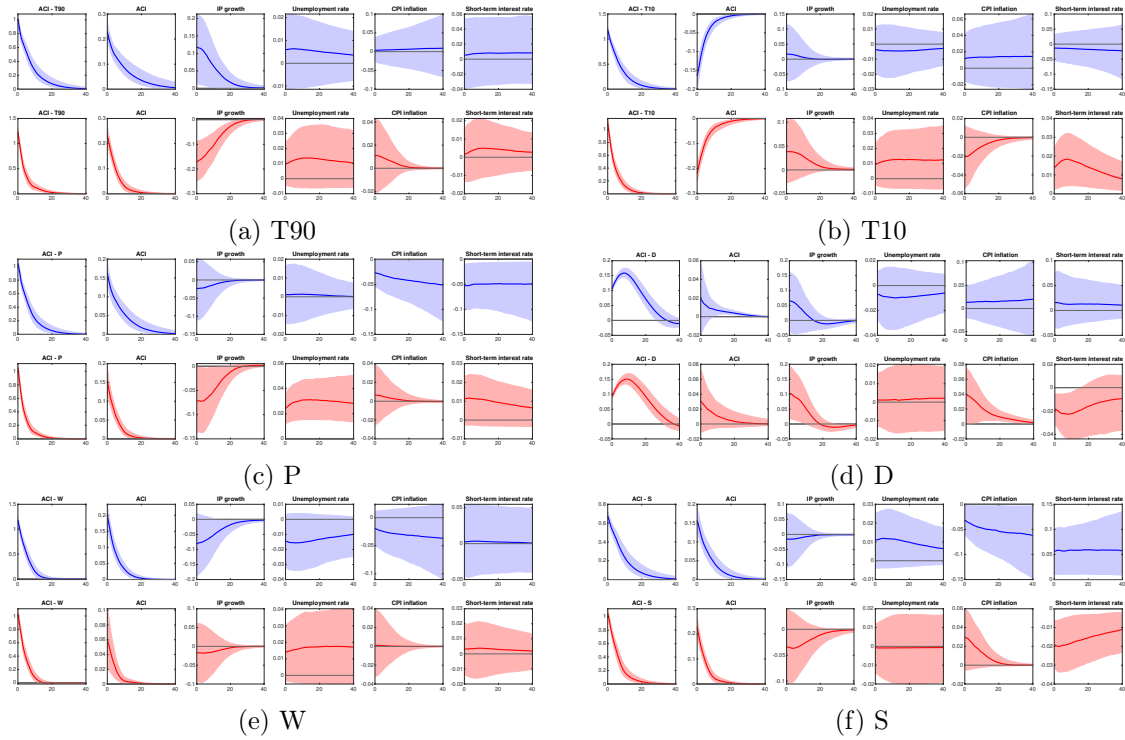
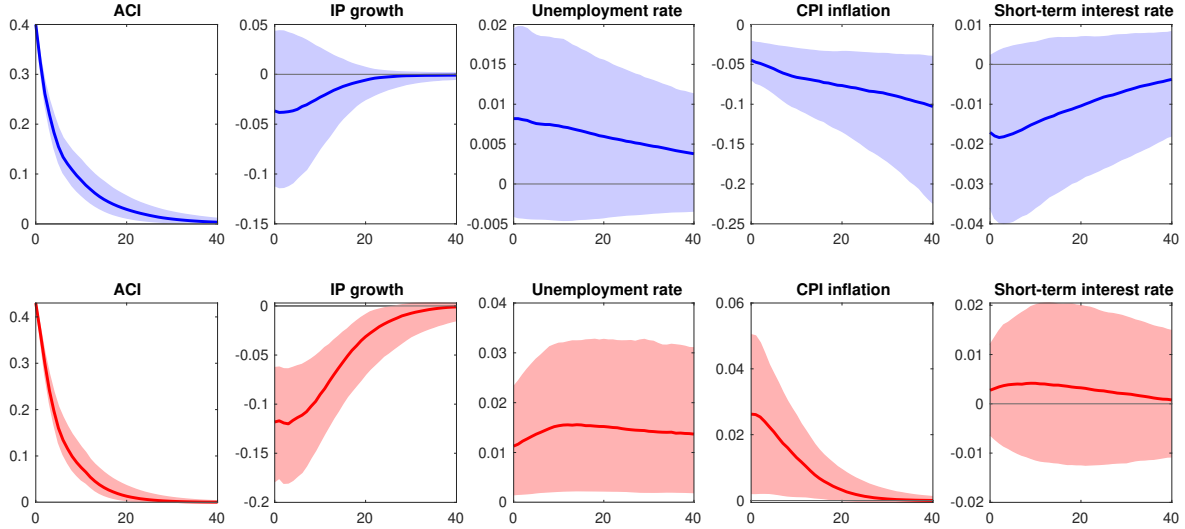
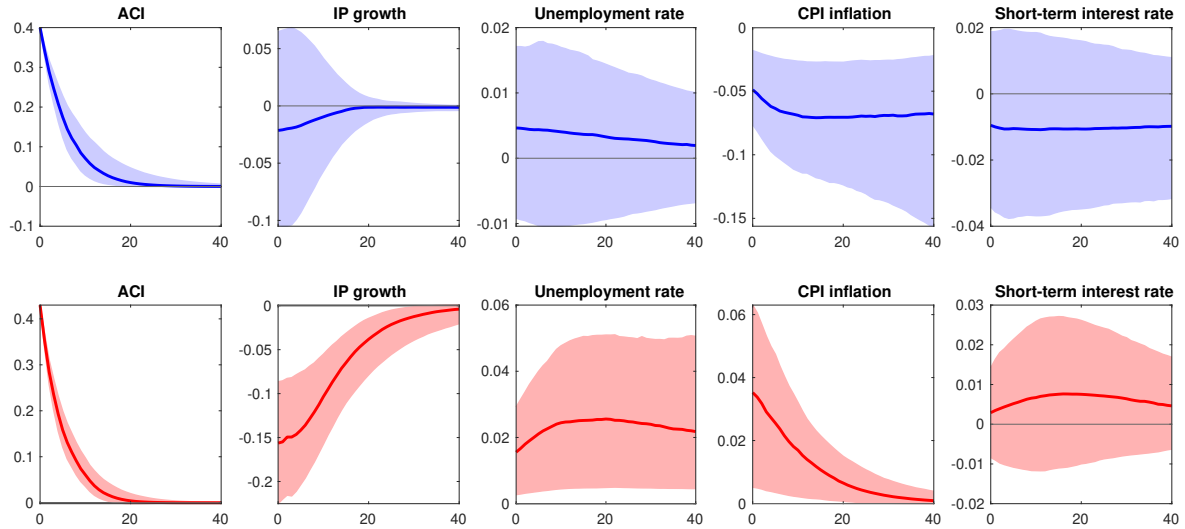


Figure A.4: Impulse responses to a one-standard-deviation shock to each ACI component. In each of the six panels, we re-estimate our benchmark model in Figure 3, but add one additional component of the ACI at a time; the additional component is ordered first. Top panels: beginning of sample ($\tilde{z}_t = 0$); bottom panels: end of sample ($\tilde{z}_t = 1$). Shaded areas represent 68% posterior bands. Horizontal axis: months after the ACI shock.



(a) Version 1: We estimate the degrees of freedom. The priors for each shock's degrees of freedom are a Gamma distribution with a mean of 3 and standard deviation of 1.



(b) Version 2: We fix the degrees of freedom a priori to 5.7.

Figure A.5: Impulse responses to a one-standard-deviation shock to the ACI assuming independent t -distributed shocks. Otherwise, the specification is the same as in Figure 3. Top panels: beginning of sample ($\tilde{z}_t = 0$); bottom panels: end of sample ($\tilde{z}_t = 1$). Shaded areas represent 68% posterior bands. Horizontal axis: months after the ACI shock.

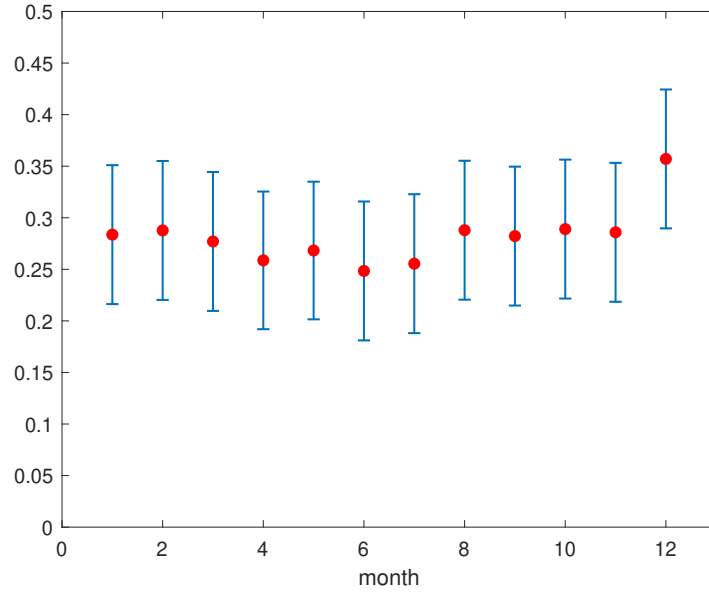


Figure A.6: Regression coefficients (red dot) of seasonally adjusted ACI on 12 monthly dummies along with the error bands (blue line) covering ± 1 standard deviation.

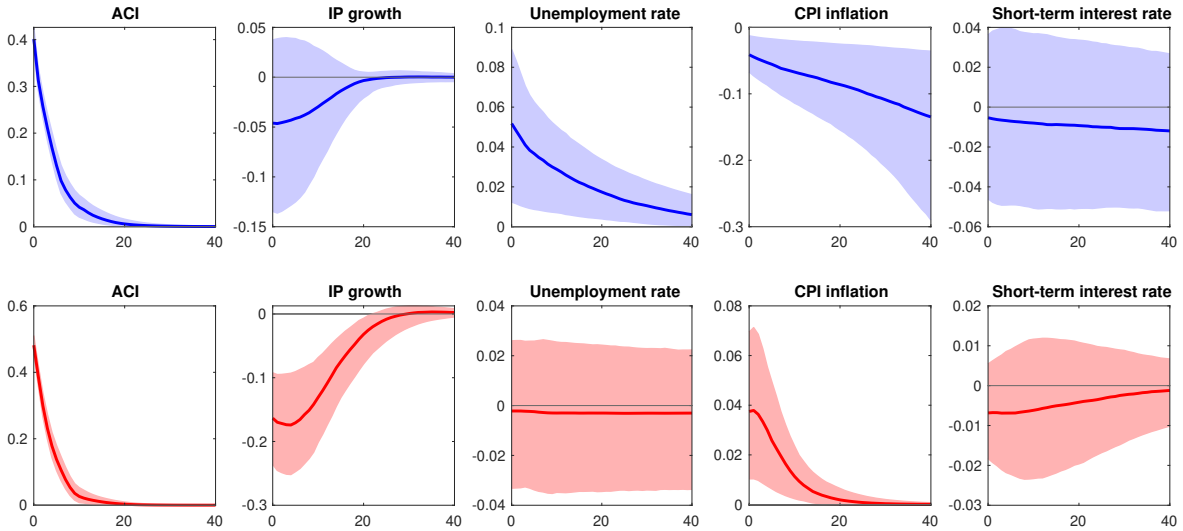


Figure A.7: Impulse responses to a one-standard-deviation shock to the ACI with non-seasonally adjusted data. Otherwise, the specification is the same as in Figure 3. Top panels: beginning of sample ($\tilde{z}_t = 0$); bottom panels: end of sample ($\tilde{z}_t = 1$). Shaded areas represent 68% posterior bands. Horizontal axis: months after the ACI shock.

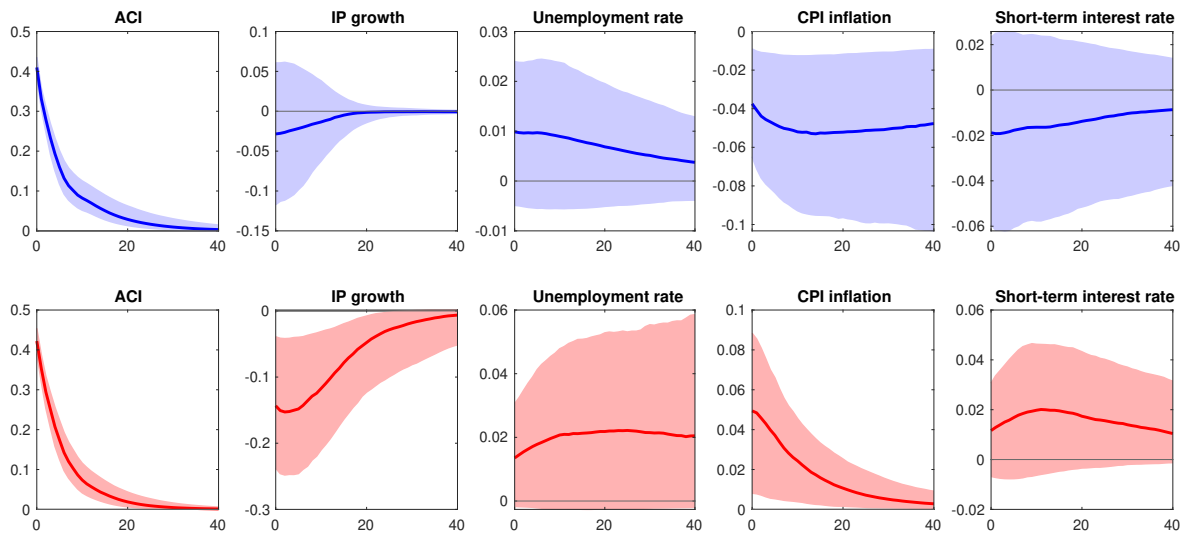
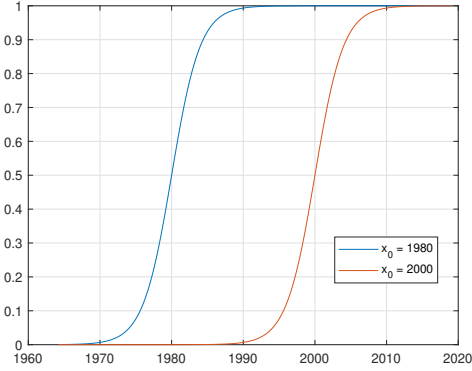
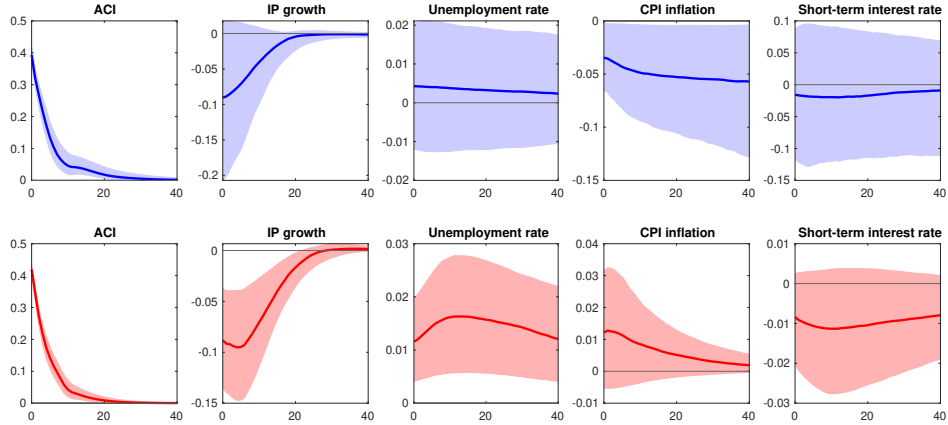


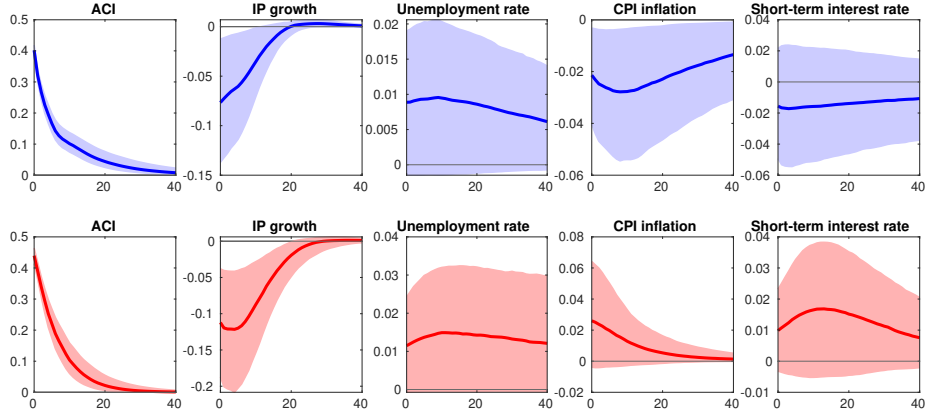
Figure A.8: Impulse responses to a one-standard-deviation shock to the ACI with lagged moving average of ACI as alternative transition. Top panels: beginning of sample ($\tilde{z}_t = 0$); bottom panels: end of sample ($\tilde{z}_t = 1$). Shaded areas represent 68% posterior bands. Horizontal axis: months after the ACI shock.



(a) Logistic functions $f(x) = \frac{L}{1+e^{-k(x-x_0)}}$, where L denotes the supremum of the values of the function, k denotes the steepness of the curve, and x_0 denotes the midpoint of the x value. We set $L = 1$, $k = 0.5$ and $x_0 \in \{1980, 2000\}$.

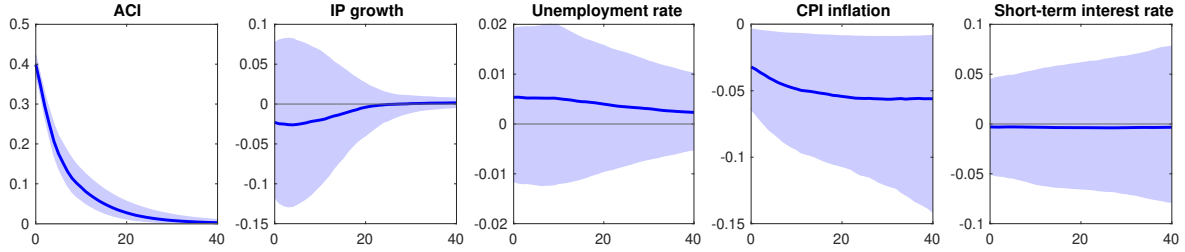


(b) Logistic function with $L = 1$, $k = 0.5$ and $x_0 = 1980$

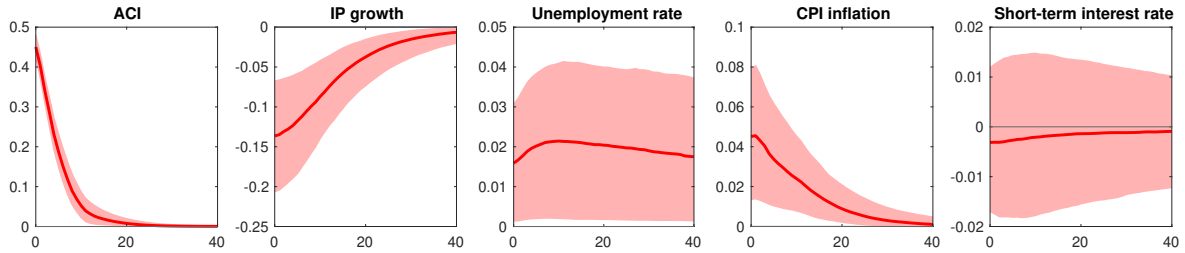
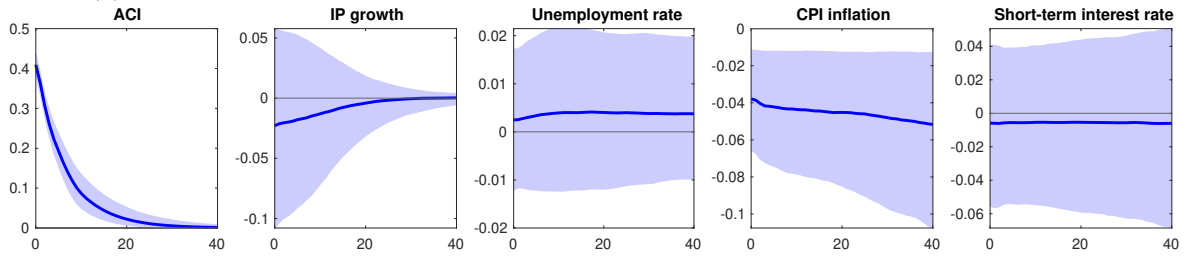
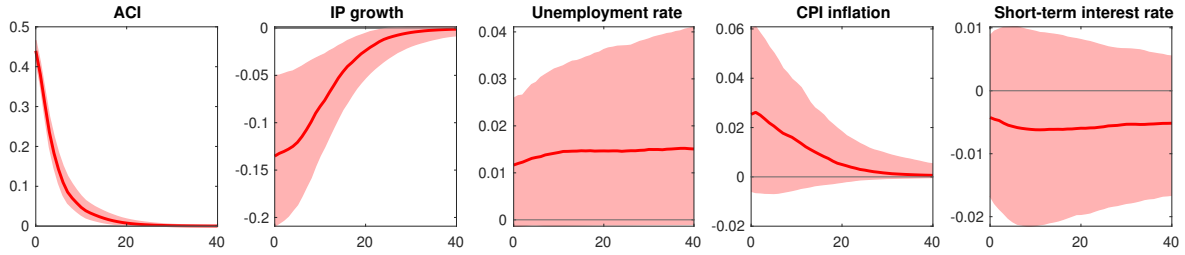


(c) Logistic function with $L = 1$, $k = 0.5$ and $x_0 = 2000$

Figure A.9: Logistic functions as alternative transition: (a) plots two logistic functions, (b) and (c) plot impulse responses to a one-standard-deviation shock to the ACI for each logistic transition. For (b) and (c), top panels: beginning of sample ($\tilde{z}_t = 0$); bottom panels: end of sample ($\tilde{z}_t = 1$). Shaded areas represent 68% posterior bands. Horizontal axis: months after the ACI shock.



(a) First principal component extracted from FRED-MD dataset as additional control.



(b) First and second principal components extracted from FRED-MD dataset as additional controls

Figure A.10: Impulse responses to a one-standard-deviation shock to the ACI when including (a) first principal component extracted from FRED-MD dataset and (b) first and second principal components extracted from FRED-MD dataset as additional controls. In this figure, we only plot responses of the benchmark variables. Top panels: beginning of sample ($\tilde{z}_t = 0$); bottom panels: end of sample ($\tilde{z}_t = 1$). Shaded areas represent 68% posterior bands. Horizontal axis: months after the ACI shock.

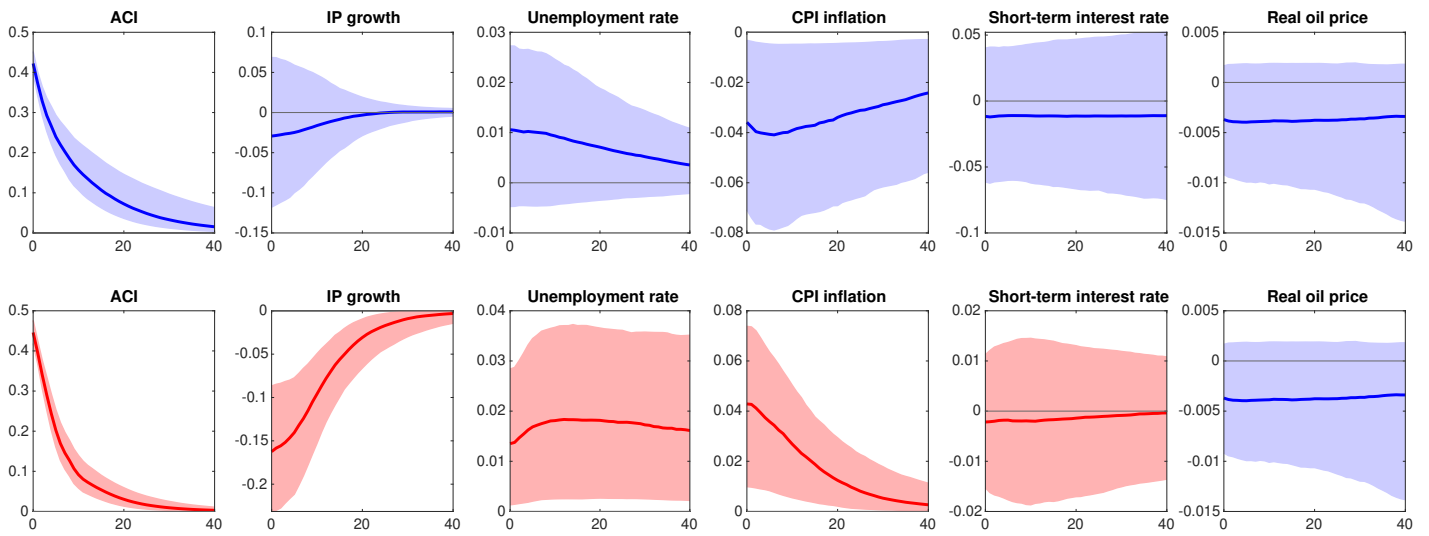


Figure A.11: Impulse responses to a one-standard-deviation shock to the ACI when including real oil price as additional control variable. Top panels: beginning of sample ($\tilde{z}_t = 0$); bottom panels: end of sample ($\tilde{z}_t = 1$). Shaded areas represent 68% posterior bands. Horizontal axis: months after the ACI shock.

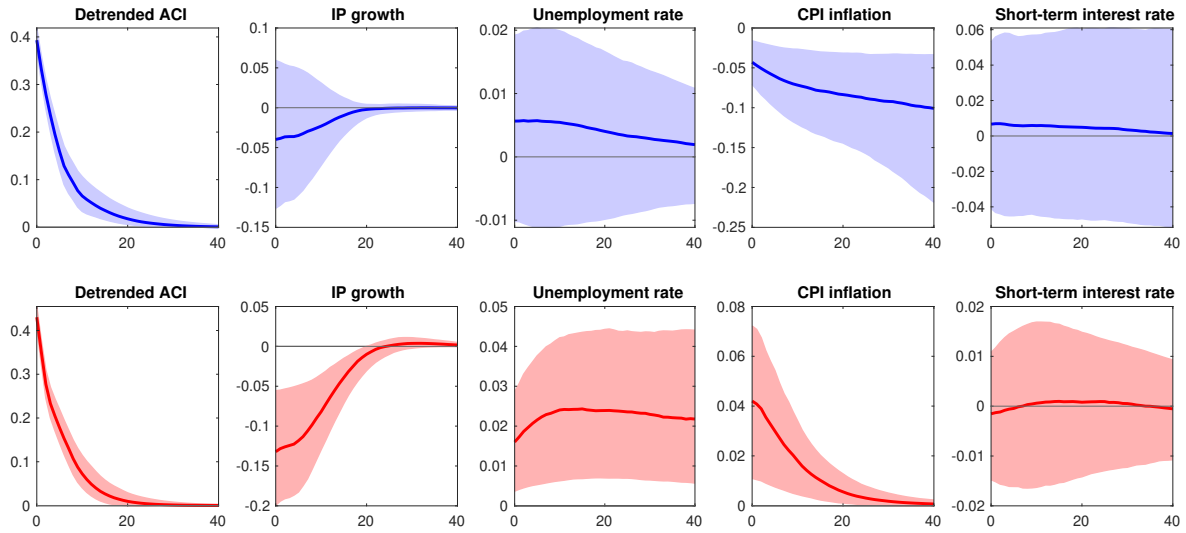


Figure A.12: Impulse responses to a one-standard-deviation shock to *detrended* ACI. Otherwise, the specification is the same as in Figure 3. Top panels: beginning of sample ($\tilde{z}_t = 0$); bottom panels: end of sample ($\tilde{z}_t = 1$). Shaded areas represent 68% posterior bands. Horizontal axis: months after the ACI shock.

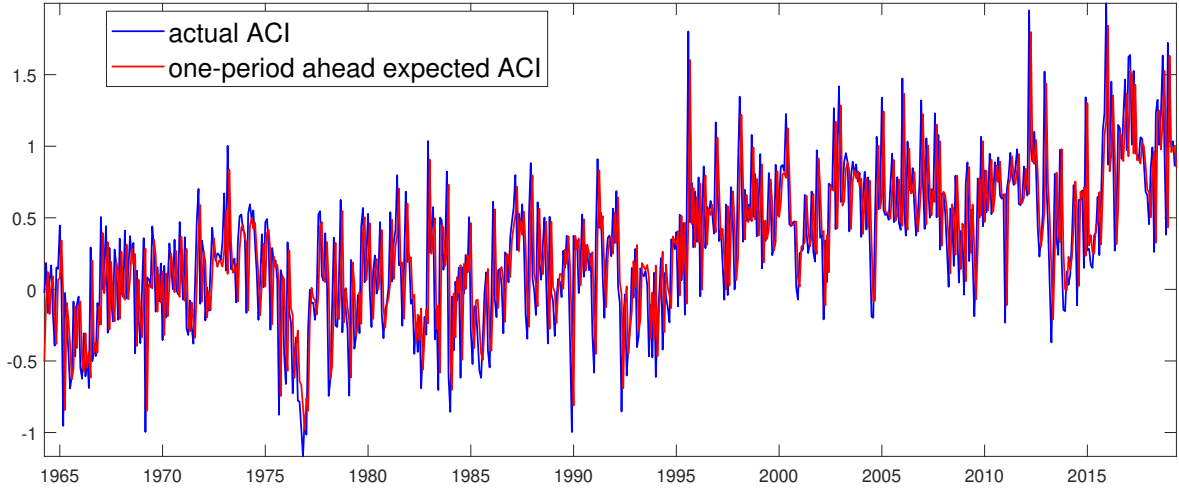


Figure A.13: Actual vs. expected ACI. The blue line plots the actual ACI and the red line plots the one period ahead expectation of ACI

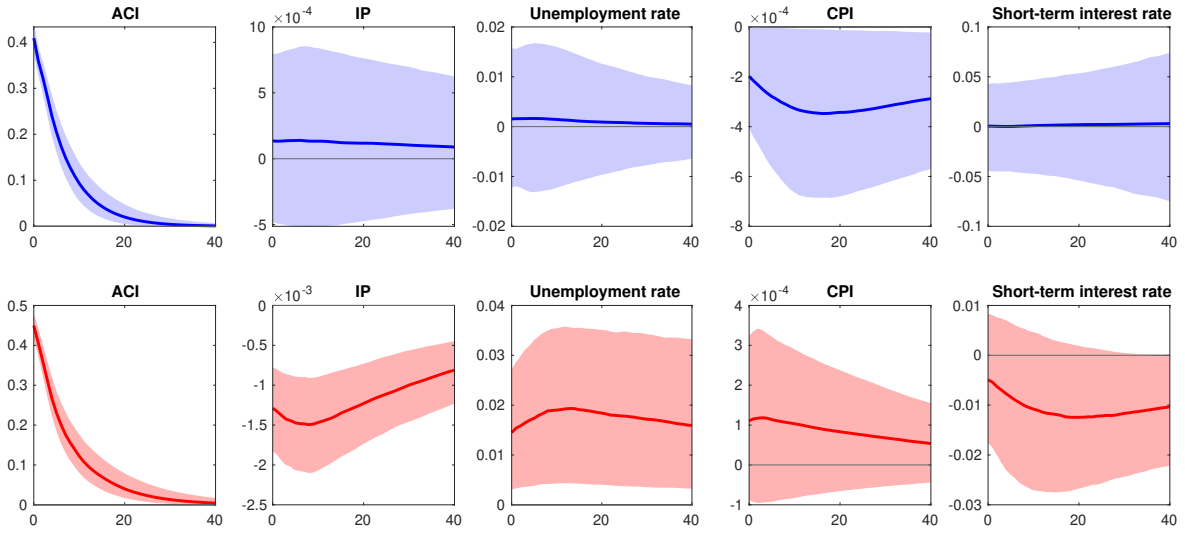


Figure A.14: Impulse responses to a one-standard-deviation shock to the ACI. In this specification, log level of IP and CPI have been used instead of growth. Top panels: beginning of sample ($\tilde{z}_t = 0$); bottom panels: end of sample ($\tilde{z}_t = 1$). Shaded areas represent 68% posterior bands. Horizontal axis: months after the ACI shock.

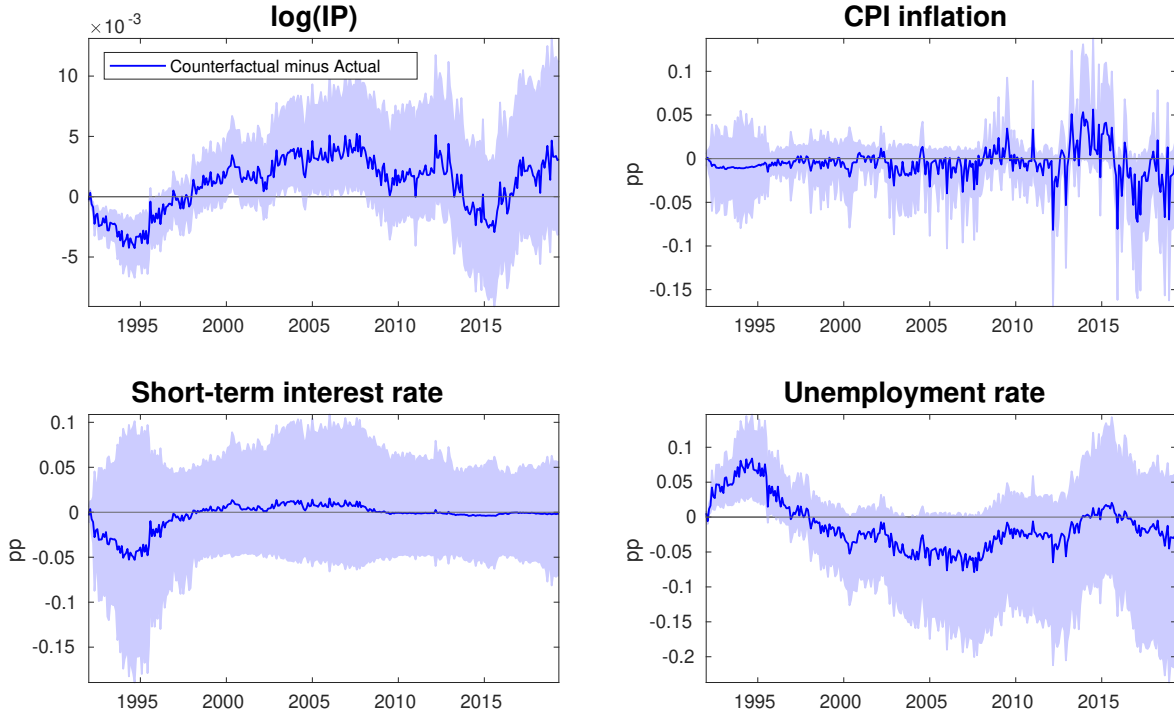


Figure A.15: Cumulative effects of ACI on macroeconomic variables since 1991m1. Each solid line plots the difference between a macroeconomic variable in the counterfactual scenario with ACI shocks set to zero and in the actual data. The shaded areas represent 68% posterior bands. The horizontal axis indicates time periods.

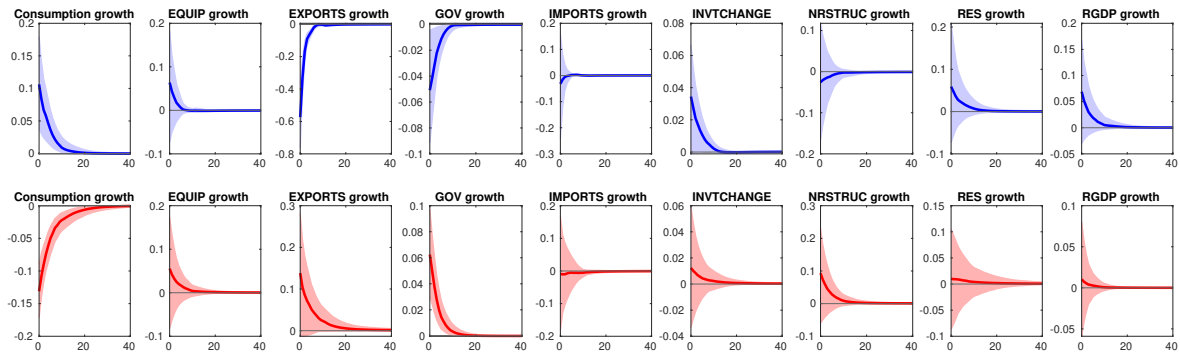
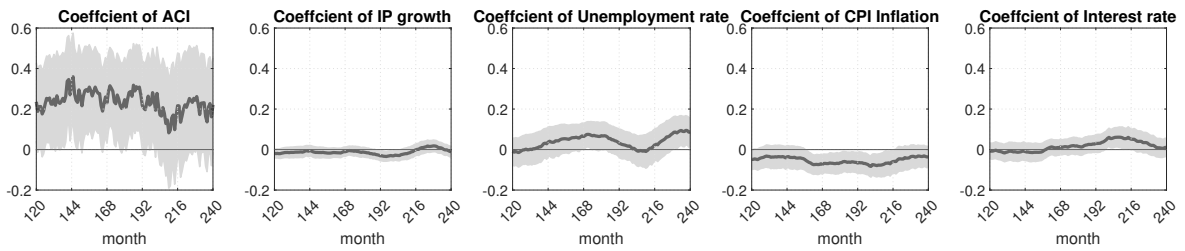
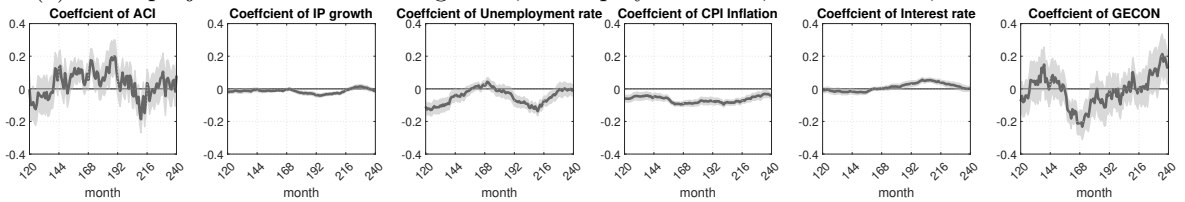


Figure A.16: Impulse responses of each component of real GDP (columns 1 to 8) and real GDP (the last column) estimated by Jarosinski and Karadi (2020) to an ACI shock. We re-estimate our benchmark model in Figure 3, but replace IP growth with each component of real GDP one at a time and present its responses in each column. Top panels: beginning of sample ($\tilde{z}_t = 0$); bottom panels: end of sample ($\tilde{z}_t = 1$). Shaded areas represent 68% posterior bands. Horizontal axis: months after the ACI shock.



(a) Local projection of ACI on IP growth, Unemployment rate, CPI inflation, and Interest rate.



(b) Local projection of ACI on IP growth, Unemployment rate, CPI inflation, Interest rate, and GECON.

Figure A.17: Each panel shows the estimated coefficients (dark gray line) of each variable in the local projections of ACI over long horizons. The shaded light gray areas represent 68% confidence bands. The horizontal axis indicates 10 years to 20 years ahead horizon.

	Top 3	Top 10	All Hurricanes	Top 20 Disasters
ACI	0.453	0.166	0.106	0.211
	(0.217)**	(0.125)	(0.057)*	(0.101)**

Table A.1: Effects of hurricane events on the ACI. The table reports the estimated coefficients and Newey-West standard errors from a regression of the ACI (first column) on the dummies for the onset months of top-3 hurricanes (first entry), top-10 hurricanes (second entry), all hurricanes (third entry), or top-20 billion-dollar disasters (last entry). Event data source: NOAA's Billion-Dollar Weather and Climate Disasters (1980-2019).